

# Physicochemical and catalytic properties of iron-promoted Raney-nickel catalysts obtained by mechanical alloying

B.H. Zeifert<sup>a</sup>, J. Salmones<sup>b,\*</sup>, J.A. Hernández<sup>a</sup>, R. Reynoso<sup>a</sup>, N. Nava<sup>b</sup>, J.G. Cabañas-Moreno<sup>a</sup> and G. Aguilar-Ríos<sup>a</sup>

<sup>a</sup> Instituto Politécnico Nacional, ESQIE, Av. IPN s/n, Edif. 7, UPALM, Zacatenco, 07300 México D.F., Mexico

<sup>b</sup> Instituto Mexicano del Petróleo, STI, Gerencia de Catálisis y Materiales, Eje Central Lázaro Cárdenas 152, 07730 México D.F., Mexico

Received 19 July 1999; accepted 11 October 1999

Raney-type catalysts were prepared by means of a two-step procedure: (i) mechanical alloying of the metals and (ii) alkaline aluminum leaching. Mechanical alloying is a novel alternative related to the synthesis of skeletal Ni catalysts. Catalysts characterization was performed by atomic absorption, X-ray diffraction, electron microscopy, and Mössbauer spectroscopies. Textural studies were also carried out. Binary Al–Ni and ternary Al–Ni–Fe alloys were produced by mechanical alloying from pure metallic powders; in particular, the intermetallic  $\beta$ -(AlNi) phase was formed with a fine microstructure as a non-equilibrium phase; then, aluminum was selectively removed. After aluminum leaching the  $\beta$ -(AlNi) phase was transformed into the more stable nickel fcc structure. The effect of iron addition to the Ni–Al catalysts depends on iron concentration and reduction temperature; both parameters determine catalysts composition and activity. This work reports physicochemical properties and benzene hydrogenation activity of these materials, compared with conventional catalysts obtained by melting and leaching.

**Keywords:** Raney-nickel, mechanical alloying, leaching, catalysts, hydrogenation

## 1. Introduction

Raney-type catalysts were first introduced in 1924; since then, these catalysts, both in powdered and granular form, have been widely applied in many commercial processes, including hydrogenation of unsaturated organic compounds, such as catalytic hydrogenation of adiponitrile to hexamethylenediamine and of benzene to cyclohexane. Also, Raney catalysts promote reductive reactions, for instance, the alkylation of carbonyl compounds with amines, the hydrogenolysis of esters and ethers, dehalogenation reactions [1], as well as fuel cell electrodes [2].

Conventional Raney-Ni catalysts (with fcc structure) are produced by removing the aluminum from binary Ni–Al alloys by leaching with an aqueous alkaline solution. These alloys are prepared by pyrometallurgical (PM) methods generally in the proportion 50:50 wt%. By this method a mixture of nickel aluminides (Al<sub>3</sub>Ni, Al<sub>3</sub>Ni<sub>2</sub>, AlNi) and Al–Al<sub>3</sub>Ni eutectic are obtained [3].

In contrast with conventional methods, mechanical alloying (MA) is a process used to produce alloys at room temperature having a fine microstructure; furthermore, it can be applied to alloy incompatible materials. Also, MA is a promising route to synthesize structural intermetallics, superplastic ceramic materials, modified semiconductor materials, protective coatings; in other words, materials with unusual structural properties [4].

Ivanov et al. [5] reported that after leaching Al atoms from  $\beta$ -AlNi structures of mechanically alloyed Ni and Co aluminides, the catalysts retained the metastable bcc struc-

ture leading to very active Ni and Co Raney-type catalysts. The bcc structure transforms into the more stable nickel fcc structure at about 463 K. In this work, MA was applied to obtain Al–Ni and Al–Ni–Fe alloys from elemental metallic powder blends. The alloys, after alkaline aluminum removal, were tested in the benzene hydrogenation reaction and compared with a conventional Raney-Ni catalyst.

## 2. Experimental

### 2.1. Catalysts preparation

Binary Al–Ni and ternary Al–Ni–Fe were prepared from powder mixtures, with nominal atomic compositions Al<sub>65</sub>Ni<sub>35</sub>, Al<sub>65</sub>Ni<sub>30</sub>Fe<sub>5</sub>, and Al<sub>75</sub>Ni<sub>15</sub>Fe<sub>10</sub> (in atomic percent). Also Al<sub>7</sub>Ni<sub>93</sub>, Al<sub>75</sub>Ni<sub>20</sub>Fe<sub>5</sub>, and Al<sub>65</sub>Ni<sub>25</sub>Fe<sub>10</sub> systems were prepared. The mixtures were milled in an attritor ball mill (Union Process, model 1-S), equipped with a water-cooled jacket and a 3.8 l stainless-steel vessel container. Stainless-steel balls (3.2 mm diameter) were used as milling media. The attritor was operated for 120 h at 350 RPM under a continuous argon gas flow. The powder charge was 100 g and the ball-to-powder weight ratio was 30:1. A volume of 20 ml of methanol was used as a surfactant agent.

Due to the pyrophoric properties of the alloyed material, in order to prevent spontaneous ignition when it is recovered from the attritor, the argon gas flow was stopped at the end of each run, and atmospheric air was allowed to contact the material; with this procedure, a slow surface oxidation

\* To whom correspondence should be addressed.

is carried out “passivating” the alloy. For the passivation step, the attritor rotation was lowered to 70 RPM.

The alloyed samples were then treated for 2 h with a 20 wt% KOH aqueous solution, held at its boiling point (digestion), in order to selectively leach away aluminum atoms; this reaction is exothermic. A passivation step as described above was necessary because the Raney-nickel catalyst thus obtained is also pyrophoric.

## 2.2. Characterization techniques

The bulk chemical composition of the materials was determined by atomic absorption spectroscopy (AA) in a Perkin–Elmer 1700 apparatus; surface composition, by electron dispersion spectroscopy (EDS) applied to large areas (250–300  $\mu\text{m}$ ), between 0.1 and 10  $\mu\text{m}$  depth depending on electron energy [6]. The materials were characterized by scanning electron microscopy (SEM) in a Jeol JSM-6300 apparatus, X-ray diffraction (XRD) experiments were carried out in a Shimadzu XD-3, using Cu  $K\alpha$  radiation, nitrogen physisorption was determined in an ASAP 2100 Micromeritics apparatus, operated at 0.2 relative pressure ( $p/p_0$ ). Pore size was estimated by means of the Kelvin equation. Iron Mössbauer spectroscopy studies (MS), were performed on a constant acceleration Austin Scientific Associates spectrometer. The  $\gamma$ -ray source was  $^{57}\text{Co}$  in a rhodium matrix. An iron foil was used as standard to evaluate Mössbauer parameters. Details are given elsewhere [7].

Catalysts activity was measured in the benzene hydrogenation reaction in a conventional continuous-flow microreactor system operated at 50 °C and atmospheric pressure with a GC on-line. Benzene was fed by saturation at 24.7 mm Hg partial pressure, with hydrogen (15.8 l/h) as carrier gas. The weight of catalyst was 0.04 g in all cases. Catalysts activation was made by a reductive treatment with hydrogen at 448 K for 10 h and at 773 K for 3 h. The lower value of reduction temperature (RT) was chosen to preserve any bcc structure that could be present in the catalysts [5].

Benzene conversion ( $X_a$ ) is defined as the percentage of benzene converted to all products. The selectivity to cyclohexane is defined as the amount of benzene converted to cyclohexane divided by the amount of reactant converted to all products, reported as mol%.

## 3. Results and discussion

### 3.1. Chemical composition (AA and EDS)

The mean compositions of the  $\text{Al}_{65}\text{Ni}_{35}$ ,  $\text{Al}_{65}\text{Ni}_{30}\text{Fe}_5$ , and  $\text{Al}_{75}\text{Ni}_{15}\text{Fe}_{10}$  alloys, after aluminum leaching and the commercial Raney-Ni are indicated in table 1.

No evidence of iron contamination from the attritor wear was observed in the binary samples.

Comparing the bulk (AA) and surface (EDS) analysis, it can be seen that after leaching, nickel is homogeneously

Table 1

Chemical composition (at%) of mechanically alloyed Al–Ni and Al–Ni–Fe systems before and after alkaline aluminum leaching compared with a conventional Raney-Ni catalyst.

Sample	AA (at%)			EDS (at%)		
	Al	Ni	Fe	Al	Ni	Fe
$\text{Al}_{65}\text{Ni}_{35}$ , leached	19	81	0	17	83	0
$\text{Al}_{65}\text{Ni}_{30}\text{Fe}_5$ , leached	14	69	17	12	70	18
$\text{Al}_{75}\text{Ni}_{15}\text{Fe}_{10}$ , leached	7	68	25	8	67	25
Conventional Raney-Ni	11	89	0	17	83	0

distributed between bulk and surface. There is no chemical reaction between iron and the leaching alkaline solution because its relative amount remains constant; besides, it is homogeneously distributed between bulk and surface.

### 3.2. Morphology of Raney-Ni catalysts (SEM)

SEM observations on the mechanical alloyed Raney-Ni catalysts showed agglomerates nearly spherical, as a typical sponge shape, with particle sizes ranging from 0.1 to 3  $\mu\text{m}$ . The conventional Raney-Ni catalyst showed a linear-shaped particle size ranging between 3 and 30  $\mu\text{m}$ . These morphologies are clearly depicted in figure 1: (a) for  $\text{Al}_{65}\text{Ni}_{35}$  leached, (b) corresponds to  $\text{Al}_{65}\text{Ni}_{30}\text{Fe}_5$  leached, compared with (c) a conventional catalyst.

### 3.3. Nitrogen physisorption

Table 2 shows textural properties of the leached alloys and the commercial catalysts obtained from nitrogen physisorption experiments. BET specific area of mechanically alloyed samples is almost three times greater compared with the commercial catalyst, which can be strongly related to the particle size distributions. On the other hand, pore size is smaller for MA samples.

### 3.4. X-ray diffraction studies (XRD)

Both mechanically alloyed samples  $\text{Al}_{65}\text{Ni}_{35}$  and  $\text{Al}_{65}\text{Ni}_{30}\text{Fe}_5$  produced similar diffraction patterns corresponding to the bcc structure of NiAl alloy ( $\beta 2$ ), as shown in figure 2(a). The formation of the  $\beta 2$  structure is probably due to the introduction of defects by the MA process, because their compositions were out of the range in which this phase is present at equilibrium conditions.

Figure 2(b) shows X-ray diffraction patterns of the  $\text{Al}_{75}\text{Ni}_{15}\text{Fe}_{10}$  system at different reduction temperatures after removing part of the aluminum atoms by leaching, including the conventional Raney-Ni catalysts. These catalysts produced XRD patterns corresponding to nickel with fcc structure. After Al removal, the crystallographic structure of the material changed from bcc to fcc structure in both binary and ternary alloys, in contrast to the results obtained by Ivanov et al. [5].

Concerning the effect of reduction temperature on the phases present ordered in decreasing importance, table 3

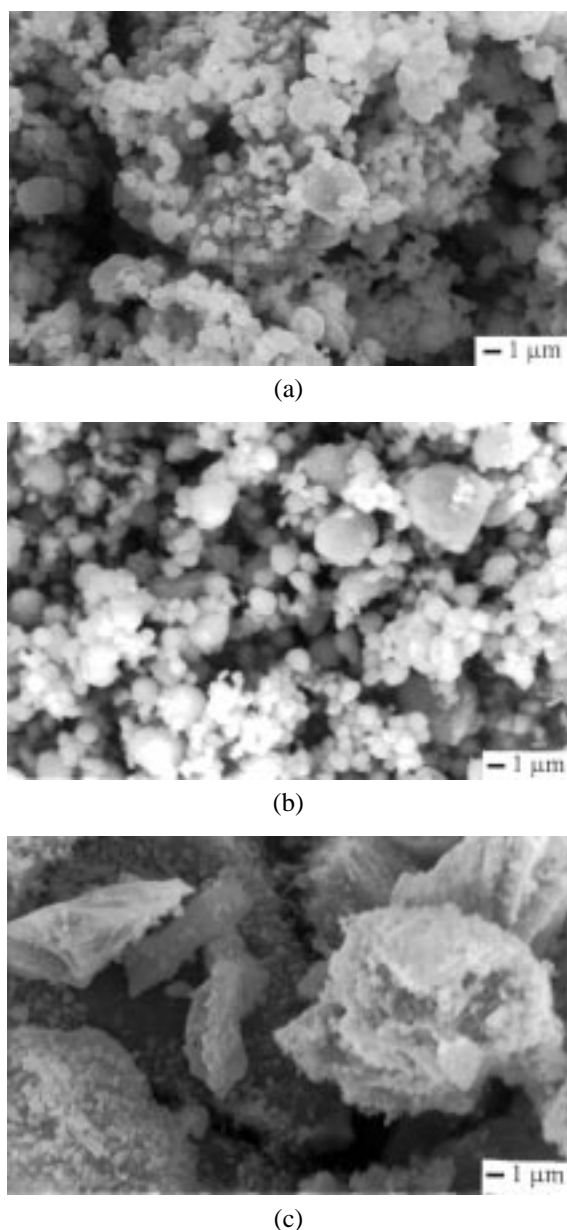


Figure 1. Scanning electron microscopy (SEM) images of mechanical alloyed catalysts: (a)  $\text{Al}_{65}\text{Ni}_{35}$ , (b)  $\text{Al}_{75}\text{Ni}_{15}\text{Fe}_{10}$ , compared with (c) a conventional Raney-Ni catalyst.

Table 2  
Textural properties of mechanically alloyed binary Ni–Al and ternary Ni–Al–Fe catalysts, compared with a conventional Raney-nickel catalyst.

Sample	Surface area ( $\text{m}^2/\text{g}$ )	Pore volume ( $\text{cm}^3/\text{g}$ )	Pore diameter ( $\text{\AA}$ )
$\text{Al}_{65}\text{Ni}_{35}$ , leached	139	0.095	27
$\text{Al}_{65}\text{Ni}_{30}\text{Fe}_5$ , leached	146	0.094	26
$\text{Al}_{75}\text{Ni}_{15}\text{Fe}_{10}$ , leached	163	0.129	32
Conventional Raney-Ni	56	0.076	54

shows a summary of XRD experiments for fresh and hydrogen-treated samples.

As shown in table 3, reduction temperature (RT), plays an important role on the composition of the catalysts. For

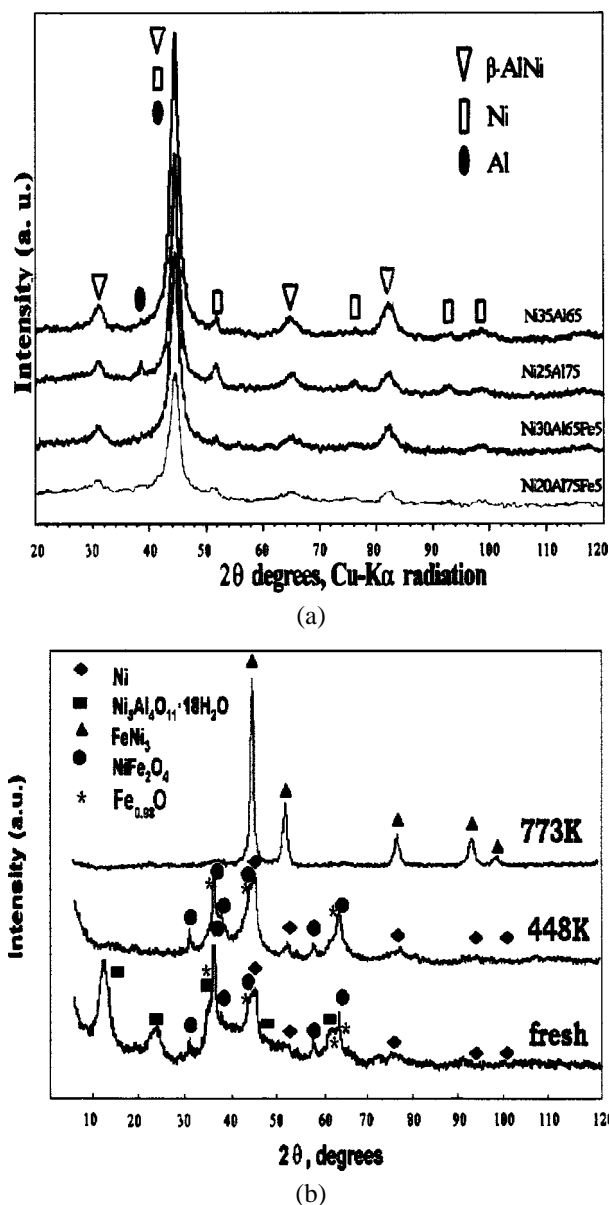


Figure 2. (a) XRD patterns of some Al–Ni and Al–Fe–Ni mechanically alloyed materials, showing the  $\beta$ -AlNi formation. (b) XRD patterns of the leached  $\text{Al}_{75}\text{Ni}_{15}\text{Fe}_{10}$  system fresh and reduced at 448 and 773 K.

bimetallic catalysts (0 at% Fe), low reduction temperatures promote Ni and hydrated Al–Ni compounds, which were not observed at 773 K RT. Concerning the Ni–Fe–Al system, the effect of RT depends on iron concentration. For 5 at% Fe, RT almost does not affect the phases present in the catalysts, nickel being the main phase present; the formation of  $\text{FeNi}_3$  compounds is also reported. Considering higher iron concentrations, low RT promotes the formation of Ni and  $\text{NiFeO}_4$  phases; when 773 K (RT) is used, all nickel present in the sample is transformed into the  $\text{FeNi}_3$  phase. In addition the  $\text{Fe}_{0.98}\text{O}$  phase (wüstite) is observed with corresponding reflections at  $2\theta$  equal to  $35.8^\circ$ ,  $38.0^\circ$ ,  $43.0^\circ$ ,  $61.0^\circ$ , and  $64.5^\circ$ , which overlaps with the  $\text{NiFe}_2\text{O}_4$  reflection at  $2\theta = 35.8^\circ$ .

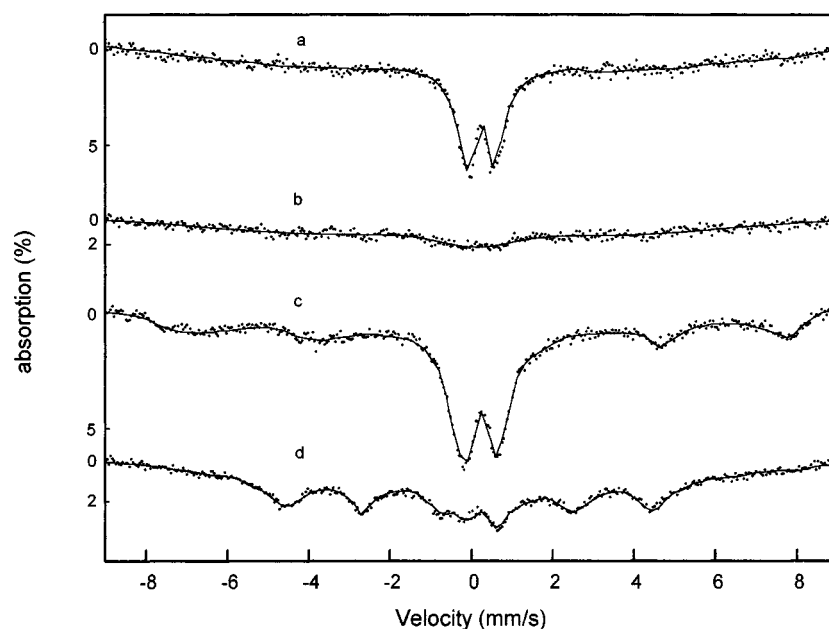


Figure 3. Iron Mössbauer spectroscopy spectra of (a) and (b) (5 at% Fe) reduced at 448 and 773 K, and (c) and (d) (10 at% Fe) reduced at 448 and 773 K, respectively.

Table 3

Effect of reduction temperature on the phases detected by XRD on Ni–Al and Ni–Al–Fe catalysts, obtained by mechanical alloying.

Sample	Fe (at%)	Reduction temperature (K)	Phase identification, XRD
Al <sub>65</sub> Ni <sub>35</sub>	0	448	Ni, Ni <sub>5</sub> Al <sub>4</sub> O <sub>11</sub> ·18H <sub>2</sub> O, Fe <sub>0.98</sub> O
Al <sub>65</sub> Ni <sub>35</sub>	0	773	Ni, NiO
Al <sub>65</sub> Ni <sub>30</sub> Fe <sub>5</sub>	5	448	Ni, NiO, FeNi <sub>3</sub> , Fe <sub>0.98</sub> O
Al <sub>65</sub> Ni <sub>30</sub> Fe <sub>5</sub>	5	773	Ni, FeNi <sub>3</sub> , NiO, NiFe <sub>2</sub> O <sub>4</sub>
Al <sub>75</sub> Ni <sub>15</sub> Fe <sub>10</sub>	10	448	NiFe <sub>2</sub> O <sub>4</sub> , Ni, Fe <sub>0.98</sub> O
Al <sub>75</sub> Ni <sub>15</sub> Fe <sub>10</sub>	10	773	FeNi <sub>3</sub>
Conventional		448	Ni, NiO
Conventional		773	Ni

### 3.5. Mössbauer spectroscopy

Before Mössbauer experiments, the samples were reduced at 448 K for 10 h and 773 K for 3 h. Mössbauer spectra are shown in figure 3. Figure 3 (a) and (b) corresponds to the low iron content samples (5 at% Fe) and figure 3 (c) and (d) to the 10 at% Fe catalysts. All of them show a central doublet near zero velocity.

Besides, NiFe<sub>2</sub>O<sub>4</sub> phase is developed (lateral peaks) [8,9] considering an increasing iron content and reduction temperature (figure 3 (a)–(c)). Regarding the 10 at% Fe catalysts, a total transformation into FeNi<sub>3</sub> (IS = 0.070 mm/s

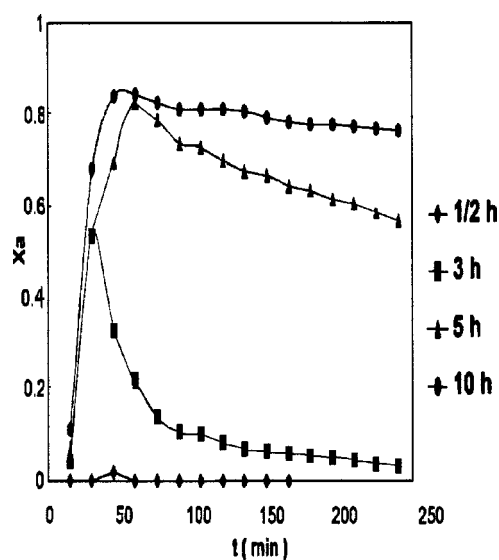


Figure 4. Effect of reduction-activation time of Al<sub>65</sub>Ni<sub>35</sub>, leached catalysts on benzene hydrogenation conversion as function of time on stream.

relative to  $\alpha$ -Fe, QS = 0.040 mm/s) phase takes place when they are reduced at 773 K (figure 3(d)). The experimental magnetic field ( $H$ ) value measured for FeNi<sub>3</sub> was 279 kOe whereas for NiFe<sub>2</sub>O<sub>4</sub> the  $H$  values were 469 kOe for iron in octahedral position and 440 kOe in tetrahedral positions, respectively. These values were compared with the literature [10,11], where they were found to be 280 kOe for FeNi<sub>3</sub> and 548 and 506 kOe for pure NiFe<sub>2</sub>O<sub>4</sub> corresponding to iron in both positions. When pure phases are considered, the agreement is better than those corresponding to mixed phases.

The central doublet near zero velocity is due to a Fe<sub>0.98</sub>O species (wüstite) with a not well defined structure repre-

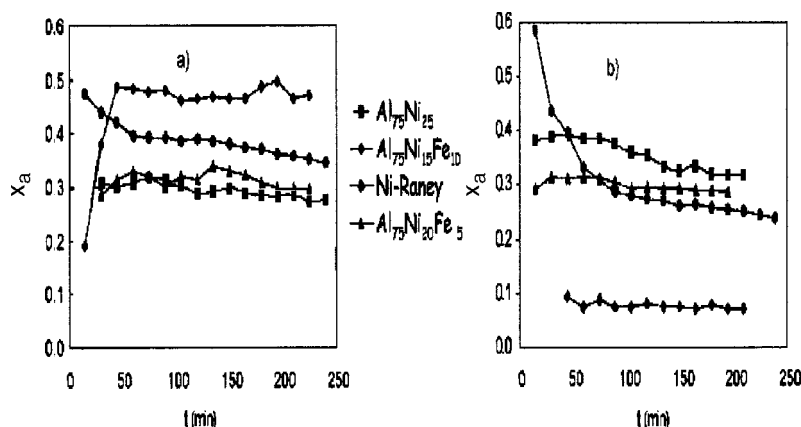


Figure 5. Benzene dehydrogenation conversion of  $\text{Al}_{75}\text{Ni}_{25}$ ,  $\text{Al}_{75}\text{Ni}_{15}\text{Fe}_{10}$ , and  $\text{Al}_{75}\text{Ni}_{20}\text{Fe}_5$  compared with a conventional Raney-Ni catalyst. Activation–reduction temperature (RT): (a) 448 and (b) 773 K.

senting almost half of the total iron present in the catalysts [12,13].

In relation to the central doublet corresponding to figure 3(b), the decrease in intensity is probably due to iron migration from  $\text{Fe}_{0.98}\text{O}$  phases to Ni phases to form  $\text{FeNi}_3$  [14].

### 3.6. Catalytic activity

#### *Effect of the reduction temperature and iron content on the activity of binary and ternary catalysts*

When the samples were reduced at 448 K, the reduction process took 10 h; whereas at 773 K, the reduction time was only 3 h, related to a complete catalyst activation. The effect of catalyst reduction time on catalyst activity at 448 K is shown in figure 4. The selectivity to cyclohexane was equal to one in all the tests.

Reduction temperature and iron content are very important: for low iron content catalysts (5 at% Fe), the reduction temperature did not affect their activity. On the other hand, when iron content was increased to 10 at% Fe, the most active catalyst was obtained for low reduction temperature (448 K), even more active than the conventional catalyst. The high iron content catalysts lost their activity when they were reduced at 773 K.

Binary Al–Ni catalysts are less active than the commercial catalysts when they are reduced at 448 K; these catalysts increase their activity when they are reduced at high temperature (773 K) (figure 5 (a) and (b)).

## 4. Conclusions

Iron-promoted Raney-Ni catalysts were produced from mechanically alloyed powders. The catalysts thus obtained show a smaller particle size distribution than a conventional catalyst obtained by pyrometallurgical methods, which can generate higher surface areas.

Reduction temperature and iron content play an important role related to surface chemistry and catalytic properties. Considering low iron concentration (5 at%), reduc-

tion temperature has a minor effect on hydrogenation activity. In these catalysts iron produces nickel compounds such as  $\text{FeNi}_3$  and  $\text{NiFe}_2\text{O}_4$  while a certain amount of free Ni phases remains responsible of catalytic activity.

The most active catalyst was found to be the 10 at% Fe reduced at low temperature (448 K); at this temperature the formation of Ni and  $\text{NiFe}_2\text{O}_4$  is favored accompanied by a promotional effect on the activity. When reduction temperature is raised to 773 K, nickel is completely transformed into  $\text{FeNi}_3$ , which is an inactive phase.

## Acknowledgement

This work has been sponsored by DEPI-IPN (project 970146), FIES-IMP (project 95-109-III) and CONACyT (4254A).

## References

- [1] R. Seymour and S. Montgomery, *Heterogeneous Catalysis*, Selected American Histories, Series 222 (Am. Chem. Soc., Washington, 1983).
- [2] W. Cheng, L.J. Czarnecki and C.J. Pereira, *Ind. Eng. Chem. Res.* 28 (1989) 1764.
- [3] P. Fouilloux, *Appl. Catal.* 8 (1983) 1.
- [4] J.S. Benjamin, *Mater. Sci. Forum* 88–90 (1992) 1.
- [5] E. Ivanov, K. Suzuki, K. Sumiyama and S. Makhlof, *Solid State Ionics* 60 (1993) 299.
- [6] L. Reimer, *Scanning Electron Microscopy* (Springer, New York, 1985) p. 3.
- [7] H. Armendáriz, G. Aguilar-Ríos, P. Salas, M.A. Valenzuela, I. Schifter, H. Arriola and N. Nava, *Appl. Catal. A* 92 (1992) 29.
- [8] J.M. Daniels and A. Rosencwaig, *Canad. J. Phys.* 48 (1970) 381.
- [9] M. De Marco, X.W. Wang, R.L. Snyder, J. Simmins, S. Bayya, M. White and M.J. Naughton, *J. Appl. Phys.* 73(10) (1993) 6287.
- [10] U. Gonser, *Mössbauer Spectroscopy* (Springer, New York, 1975) p. 229.
- [11] N.N. Greenwood and T.C. Gibb, *Mössbauer Spectroscopy* (Chapman and Hall, London, 1971) pp. 248, 266.
- [12] H. Topsøe, J.A. Domesic and M. Boudart, *J. Catal.* 28 (1973) 477.
- [13] S. Yunes, D.S. Thakur, P. Grange and B. Delmon, *Catalysis in Petroleum Refining* (Elsevier, Amsterdam, 1990) p. 317.
- [14] B. Window, *J. Appl. Phys.* 44 (1973) 2853.